JOC*Article*

Thiolytic Chemistry of Alternative Precursors to the Major Metabolite of the Cancer Chemopreventive Oltipraz[1]

Mettachit Navamal,[†] Colleen McGrath,[†] Jennifer Stewart,[†] Patrick Blans,[†] Frederick Villamena,[‡] Jay Zweier,[‡] and James C. Fishbein*[,†]

Department of Chemistry and Biochemistry, University of Maryland, Baltimore County, 1000 Hilltop Circle, Baltimore, Maryland 21250, and EPR Center, Johns Hopkins Allergy and Asthma Center, 5501 Hopkins Bayview Circle, Baltimore, Maryland 21240

jfishbei@umbc.edu

Received September 6, 2002

The compounds 7-methyl-6,8-bis(methyldisulfanyl)pyrrolo[1,2-*a*]pyrazine (**5**; "bis disulfide") and methanethiosulfonic acid *S*-((6-(methanesulfonylsulfanyl)-7-methyl)pyrrolo[1,2-*a*]pyrazin-8-yl) ester (**6**; "bis methanesulfonic acid thioester") have been synthesized to serve as alternative precursors to the major metabolite, **4**, of the cancer chemopreventive oltipraz, **1**, to test whether they possess similar biological activities. In the present work the mechanisms by which these compounds react with glutathione have been investigated in order to validate the assumption that they would be chemically competent in the presence of the biological thiols to give the oltipraz metabolite. A kinetic and product study was carried out in mainly aqueous media, ≤15% ethanol by volume, at 37 °C. The kinetic analysis and identification of intermediates by electrospray HPLC/MS indicate that compound **5** decomposes in two sequential reactions via thiol−disulfide interchange involving removal of the two thiomethyl groups. In contrast, **6** decomposes in three sequential steps, the first entailing formation of the diglutathionyl adduct, followed by two subsequent thiol disulfide interchange reactions involving loss of the glutathionyl moieties. Both **5** and **6**, as well as oltipraz itself, give nearly quantitative yields of the metabolite **4** in reactions with glutathione. Analysis of the decay of **6** by EPR spin trapping methods indicates that less than 0.2% of the reaction flux proceeds through radicals more stable than the hydroxyl radical.

Introduction

We are currently engaged in trying to understand the molecular basis for the cancer chemopreventive action of 1,2-dithiole-3-thiones.[2−5] A member of this class of compounds, oltipraz, **1**, is currently in phase 2 clinical trials as a protective agent against environmentally induced hepatocellular carcinoma.[6−8] The biochemical basis for the action of these and a number of other cancer chemopreventive agents is becoming increasingly clear.[9−15] Such compounds appear to act in part by increasing the levels of the "phase 2" enzymes of xenobiotic metabolism—a group of enzymes involved in electrophile trapping and conjugation for export.

The molecular basis by which the increased transcription of phase 2 enzymes is mediated is not clear. In essence two hypotheses have been invoked. The first posits that oltipraz or some metabolite therefrom acts as an electrophile at a protein thiol or dithiol that is, or controls the action of, a transcription mediator, thereby

[†] University of Maryland.

[‡] Johns Hopkins Allergy and Asthma Center.

(1) This work was supported by The National Institutes of Health, National Cancer Institute, through Grant RO1 CA91032.

(2) Clapper, M. L. *Pharmacol. Ther.* **1998**, *78*, 17−27.

(3) Ansher, S. S.; Dolan, P.; Bueding, E. *Food Chem. Toxicol.* **1986**, *24*, 405−415.

(4) Kensler, T. W.; Groopman, J. D.; Sutter, T. R.; Curphey, T. J.; Roebuck, B. D. *Chem. Res. Toxicol.* **1999**, *12*, 113−126.

(5) Wilkinson, J.; Clapper, M. L. *Proc. Soc. Exp. Biol. Med.* **1997**, *216*, 192−200.

(6) Camoirano, A.; Bagnasco, M.; Bennicelli, C.; Cartiglia, C.; Wang, J. B.; Zhang, B. C.; Zhu, Y. R.; Qian, G. S.; Egner, P. A.; Jacobson, L. P.; Kensler, T. W.; De Flora, S. *Cancer Epidemiol., Biomarkers Prev.* **2001**, *10*, 775−783.

(7) Jacobson, L. P.; Zhang, B. C.; Zhu, Y. R.; Wang, J. B.; Wu, Y.; Zhang, Q. N.; Yu, L. Y.; Qian, G. S.; Kuang, S. Y.; Li, Y. F.; Fang, X.; Zarba, A.; Chen, B.; Enger, C.; Davidson, N. E.; Gorman, M. B.; Gordon, G. B.; Prochaska, H. J.; Egner, P. A.; Groopman, J. D.; Munoz, A.; Helzlsouer, K. J.; Kensler, T. W. *Cancer Epidemiol., Biomarkers Prev.* **1997**, *6*, 257−265.

(8) Kensler, T. W.; He, X.; Otieno, M.; Egner, P. A.; Jacobson, L. P.; Chen, B.; Wang, J. S.; Zhu, Y. R.; Zhang, B. C.; Wang, J. B.; Wu, Y.; Zhang, Q. N.; Qian, G. S.; Kuang, S. Y.; Fang, X.; Li, Y. F.; Yu, L. Y.; Prochaska, H. J.; Davidson, N. E.; Gordon, G. B.; Gorman, M. B.; Zarba, A.; Enger, C.; Munoz, A.; Helzlsouer, K. J.; et al. *Cancer Epidemiol., Biomarkers Prev.* **1998**, *7*, 127−134.

(9) Benson, A. B. *J. Cell Biochem. Suppl.* **1993**, *17F*, 278−291.

(10) Wang, J. S.; Shen, X.; He, X.; Zhu, Y. R.; Zhang, B. C.; Wang, J. B.; Qian, G. S.; Kuang, S. Y.; Zarba, A.; Egner, P. A.; Jacobson, L. P.; Munoz, A.; Helzlsouer, K. J.; Groopman, J. D.; Kensler, T. W. *J. Natl. Cancer Inst.* **1999**, *17*, 347−354.

(11) Egner, P. A.; Kensler, T. W.; Prestera, T.; Talalay, P.; Libby, A. H.; Joyner, H. H.; Curphey, T. J. *Carcinogenesis* **1994**, *15*, 177−181.

(12) Prochaska, H. J.; Talalay, P. *Cancer Res.* **1988**, *48*, 4776−4782.

(13) Davidson, N. E.; Egner, P. A.; Kensler, T. W. *Cancer Res* **1990**, *50*, 2251−2255.

(14) Kensler, T. W.; Primiano, T.; Sutter, T. R.; Egner, P. A.; Dolan, P. M.; Groopman, J. D.; Curphey, T. J.; Roebuck, B. D. *Proc. Int. Symp. Nat. Antioxid.* **1996**, 243−250.

(15) Maxuitenko, Y. Y.; Libby, A. H.; Joyner, H. H.; Curphey, T. J.; MacMillan, D. L.; Kensler, T. W.; Roebuck, B. D. *Carcinogenesis* **1998**, *19*, 1609−1615.

10.1021/jo020588n CCC: $22.00
Published on Web 11/28/2002

altering its activity.[4] The second hypothesis posits that reactive oxygen species (ROS) that are formed in the reactions of dithiolethiones with thiols and metal ions activate redox active transcription factors.[16]

The human metabolism of oltipraz was studied some time ago as it has been previously employed as an antischistosomal agent and is described in part of eq 1.[17] A small amount, 1%, is converted to the oxo analogue, **2**, itself a phase 2 enzyme inducer,[15,18] but the major portion is converted to the dimethylated product, **3**, which is further metabolized to a number of glucuronic acid conjugates. The compound **3** presumably arises from biological methylation of the pyrrolopyrazine, **4**, which Fleury has shown is formed by the reaction of thiolates with oltipraz.[19,20]

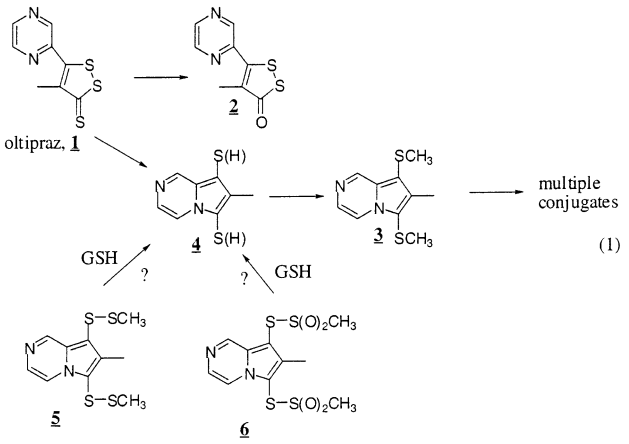

The observation that compound **3** is not a phase 2 enzyme inducer[18] means that, despite the complex metabolism of oltipraz, only three agents can be considered likely candidates as the active species that mediate the phase 2 enzyme induction: **1**, its oxo analogue, **2**, and the intermediate **4**. We do not rule out possible intermediates between **1** and **4**, but consider them less likely.

In an effort to clarify the molecular basis of phase 2 enzyme induction, we seek to characterize the electrophilic and ROS-generating potential of these three species. We report here the synthesis and characterization of 7-methyl-6,8-bis(methyldisulfanyl)pyrrolo[1,2-*a*]pyrazine (**5**; "bis disulfide") and methanethiosulfonic acid *S*-((6-(methanesulfonylsulfanyl)-7-methyl)pyrrolo[1,2-*a*]-pyrazin-8-yl) ester (**6**; "bis methanesulfonic acid thioester"), in essence putative "prodrugs" for the delivery of intermediate **4**, independent of oltipraz. A prodrug approach was adopted because it was assumed that intermediate **4** would be ionized to some degree at physiological pH, thus inhibiting its absorption in cells and a direct test of **4** as a phase 2 enzyme inducer. As reported within, compounds **5** and **6** react readily, but by different mechanisms, with the biological thiol glutathione at physiologically relevant pH and GSH concentrations to give the intermediate **4** in nearly quantitative yield.

Experimental Section

Materials. Oltipraz was a generous gift of Dr. James Crowell, Chemoprevention Branch, National Cancer Institute, NIH. All other reagents were obtained from commercial sources and typically ACS grade or better.

Synthesis. (a) 7-Methyl-6,8-bis(methyldisulfanyl)pyrrolo[1,2-*a*]pyrazine (5). A 5 equiv amount of sodium thiomethoxide was added to a 50 mL ethanolic suspension of 300 mg of oltipraz. Within 1 min, the cloudy, bright orange suspension clarified to an orange-brown solution. The mixture was allowed to stir for 30 min. A 7 equiv amount (to oltipraz) of methyl methane thiol sulfonate (MMTS) was added, and the reaction was stirred for 1 h. Within a few minutes of addition of MMTS, the solution turned yellow, and after 30 min, the reaction became milky orange. Ethanol was removed, and the crude product was placed under high vaccuum for 24 h. The orange solid was resuspended in 10 mL of chloroform and filtered. Chloroform was removed from the filtrate by rotary evaporation; the product was redissolved in 4 mL of boiling ethanol and allowed to recrystallize at room temperature in the dark. Spectral data: UV (EtOH) λ_{max} 227 nm (ϵ 19 900), 266 nm (ϵ 20 900), 351 nm (ϵ 5600); ^{1}H NMR (300 MHz, $CDCl_3$) δ 9.08 (d, 1H, J = 1.50 Hz), 8.24 (dd, 1H, J = 1.50, 4.76 Hz), 7.82 (d, 1H, J = 4.76 Hz), 2.57 (s, 3H), 2.48 (s, 6H); ^{13}C NMR (300 MHz, $CDCl_3$) δ 142.61, 137.16, 132.55, 129.04, 116.26, 115.11, 107.88, 22.48, 22.22, 10.50. Anal. Calcd for $C_{10}H_{12}N_2S_4$: C, 41.64; H, 4.19; N, 9.71. Found: C, 41.79; H, 4.13; N, 9.74.

(b) Methane Thiosulfonic Acid *S*-((6-(Methanesulfonylsulfanyl)-7-methyl)pyrrolo[1,2-*a*]pyrazin-8-yl) Ester (6). A 4 equiv amount of sodium thiomethoxide was reacted with 200 mg of oltipraz in 20 mL of an argon-flushed methanolic solution for 1.5 h. The reaction transformed from a bright orange-red suspension to a clear orange-red solution. Methanol was removed by heating the reaction in a 35 °C water bath under an argon stream. The reaction was further dried in vacuo for a 1 h. A 20 mL volume of acetonitrile was added and maintained under an argon atmosphere. The reaction solution was cooled to −15 °C before 0.34 mL of methyl sulfonyl chloride was added dropwise and allowed to stir for 20 h at room temperature. The suspension changed from reddish-brown to a pale orange color overnight. The solvent was removed in vacuo, and the solid was partially dissolved in 40 mL of dichloromethane. The suspension containing orange-brown solids was filtered. Silica gel (5 gm) was mixed into the dichloromethane filtrate, and the solvent was removed in vacuo. The product incorporated in the silica gel was packed onto the top of a silica gel column and purified using 60/40 CH_2Cl_2/EtOAc (v/v) as the eluant. A yellow fraction (R_f = 0.4 on thin layer chromatography (TLC), 100% ethyl acetate) was collected and dried to solid. The solid was recrystallized in CH_2Cl_2. The crystals were dried under high vacuum; extended drying (3 days) failed to remove all CH_2Cl_2 as indicated by ^{1}H NMR. The molar equivalents of residual solvent indicated by ^{1}H NMR were in agreement with the elemental analysis indicated. Spectral data: UV (MeCN) λ_{max} 268 nm (ϵ 17 000), 327 nm (ϵ 7500); ^{1}H NMR (300 MHz, $CDCl_3$) δ 9.14 (s, 1H), 8.46 (dd, 1H, J = 1.1, 4.76 Hz), 8.03 (d, 1H, J = 4.76 Hz), 3.22 (s, 3H), 3.19 (s, 3H), 2.63 (s, 3H); ^{13}C NMR (300 MHz, $CDCl_3$) δ 142.3, 141.7, 133.9, 131.0, 117.1, 109.4, 99.8, 48.0, 47.6, 10.9. Anal. Calcd for $C_{10}H_{12}N_2S_4O_4$·(0.1 mol CH_2Cl_2): C, 33.61; H, 3.41; N, 7.76. Found: C, 33.48; H, 3.35; N, 7.70.

(c) 7-Methyl-6,8-bis(methylsulfanyl)pyrrolo[1,2-*a*]pyrazine (3). A 250 mg amount of oltipraz was dissolved in 70 mL of 50/50 (v/v) aqueous 0.01 M ammonium acetate/MeOH solution. To this was added 780 mg of sodium thiomethoxide, and the reaction was allowed to proceed for 2.5 h. The bright orange suspension turned orange-red and became more vis-

(16) Kim, W.; Gates, K. S. *Chem. Res. Toxicol.* **1997**, *10*, 296−301.
(17) Bieder, A.; Decouvelaere, B.; Gaillard, C.; Depaire, H.; Heusse, D.; Ledoux, C.; Lemar, M.; LeRoy, J. P.; Raynaud, L.; Snozzi, C.; Gregoire, J. *Arzneim.-Forsch.* **1983**, *33*, 1289−1297.
(18) O'Dwyer, P. J.; Clayton, M.; Halbherr, T.; Myers, C. B.; Yao, K. *Clin. Cancer Res.* **1997**, *3*, 783−791.
(19) Fleury, M. B.; Largeron, M. *Tetrahedron* **1985**, *41*, 3705−3715.
(20) Largeron, M.; Martens, T.; Fleury, M. B. *Tetrahedron Lett.* **1987**, *43*, 3421−3428.

cous. Methyl iodide (1.2 g) was added, and the reaction turned orange within 30 s after the addition. The solution clarified within 10 min and was allowed to react for an additional 2 h. The product was extracted with ethyl acetate and washed with saturated sodium chloride solution. The ethyl acetate, after drying with sodium sulfate, was removed in vacuo. The yellow solid was dissolved in 20 mL of ethanol. The product was purified by semipreparative HPLC using an isocratic elution by 70/30 MeOH/H_2O on a Phenomenex Luna 5μ C(18)2 250 × 21.2 mm column. The product was collected at 40 min and dried, in vacuo, to a light yellow solid. Purity was confirmed by ^{1}H NMR and elemental analysis and is consistent with published data.[19,20] ^{1}H NMR (300 MHz, $CDCl_3$) δ 8.97(d, 1H, J = 1.10 Hz), 8.19 (dd, 1H, J = 1.1, 4.76 Hz), 7.69 (d, 1H, J = 4.76 Hz), 2.50 (s, 3H), 2.35 (s, 3H), 2.28 (s, 3H); ^{13}C NMR (300 MHz, $CDCl_3$) δ 142.6, 135.4, 130.7, 127.9, 115.7, 107.6, 19.9, 17.3, 10.1. Anal. Calcd for $C_{10}H_{12}N_2S_2$: C, 53.56; H, 5.40; N, 12.50. Found: C, 53.55; H, 5.36; N, 12.50.

Kinetics. Kinetic experiments were performed at 37 °C on a standard UV−visible spectrophotometer and a stopped-flow spectrophotometer. Reactions were initiated by addition of substrate after temperature equilibration. Typical substrate concentrations were ~60 μM and [GSH] > 0.001 M. The final reaction conditions for **5** were 1 mM EDTA, 0.01−0.05 M buffer, and 15% ethanol by volume and ionic strength = 0.1 M. The final reaction conditions for **6** were 1 mM EDTA, 0.01−0.05 M buffer, and 4% acetonitrile by volume. Values of pH for reactions were recorded at the end of the reactions at 37 °C and were used without corrections of any kind.

Product Analyses. Product analysis was carried out by an indirect method in which the reaction product (**4**, eq 1) was methylated (to give **3**, eq 1) and quantified by means of HPLC separation and UV/vis detection. A chromatography system with diode array detection and vendor software was used for analysis. The product **3** was separated from the reaction solution by use of a Phenomenex Luna C-18 column (250 × 4.6 mm). A gradient of 100% aqueous 25 mM ammonium acetate from 0 to 5 min followed by a linear change to 100% methanol from 15 to 25 min was employed for the separation, the methylated product **3** eluting at 14.6 min with a flow rate of 1 mL/min. Typically for **5** and **6**, the reaction was allowed to proceed to endpoint, reaction conditions generally as described in the kinetic runs (above). A 3 mL reaction volume was employed, and, at endpoint, 3 μL of CH_3I was added to the stirred reaction solution and the methylation reaction proceeded for 50 min. An initial time course study indicated that at pH = 7, the methylated product was maximal after 50 min and did not decrease after up to 100 min. Analyses were performed in triplicate. Yields were based on the gravimetrically determined amount of **5** and **6** and on standard curves generated with the authentic **3**. In the case of the product of oltipraz decomposition, this much slower reaction was quenched well before completion and the extent of reaction, typically 50−70%, was quantified by the decrease of oltipraz. The reported yields were calculated on the basis of the percent of oltipraz that had undergone reaction.

Mass Spectrometry. The intermediates and the products of the reactions of **5** and **6** with GSH were analyzed on a HPLC spectrometer equipped with a photodiode array detector and a mass spectrometer. The mass spectrometer conditions were electrospray negative ion mode with the source temperature set at 125 °C, desolvation temperature at 325 °C, cone voltages between 10 and 80 V, cone gas flow at ca. 73 L/h, and the desolvation gas flow at ca. 376 L/h. Separations were performed using a Phenomenex Luna 3μ C18(2) 150 × 2 mm column at a flow rate of 0.15 mL/min.

EPR Measurements. EPR measurements were carried out on an X band spectrometer with HS resonator at room temperature. General instrument settings are as follows: microwave power, 10 mW; modulation amplitutude, 1.0 G; receiver gain, (3.17−3.56) × 10^5; scan time, 84 s; time constant, 328 ms; center field, 3507.9 G; sweep width, 123.0 G. Measurements were performed in a flow-through sample cell. Typically **6** was added last (final concentration of 50−100 μM) to a solution containing 50 mM phosphate buffered saline, pH = 7.0, 1 mM GSH, and 20 mM 5,5-dimethyl-1-pyrroline-*N*-oxide (DMPO), 4% acetonitrile by volume. Spectra were accumulated over 10 min at 1 scan/min. Background was recorded using solutions containing all other reagents except **6**.

TABLE 1. Yields of Derivative 3 Following Decomposition at 37 °C by Glutathione of Oltipraz (1), 5, and 6 and Subsequent Methylation by CH_3I[a]

compd	% yield, pH = 5.0 [b]	% yield, pH = 7.0 [c]
1[d]		91 ± 1[e]
5[f,g]	97 ± 2	97 ± 4[e]
6[f]	93 ± 2	92 ± 2

[a] See eq 1 for compound structures. Reactions were 15 mM in GSH 0.05 M buffer, initiated by substrate addition and quenched by addition of CH_3I (see Experimental Section). For a given experiment, the yields were based on triplicate injections. [b] Acetate buffer. [c] Tris buffer. [d] Yield based on between 50 and 70% reaction determined by disappearance of oltipraz. Reactions contained 15% ethanol by volume. [e] Average and standard deviation of two determinations. [f] Yield after more than 10 half-lives of reaction. [g] Reactions contined15% ethanol by volume.

Results

Final Product. Although, as detailed within, both **5** and **6** react with GSH in a series of steps, the final stable product in each case appears by UV/vis spectroscopy to be qualitatively identical and also identical to the major product of the reaction of GSH with olitpraz. Fleury had earlier reported the major product from reaction of oltipraz with thiolates in basic ethanol, after derivatization by methylation, to be the compound **3**.[19,20] We chose to quantitate **3,** after methylation as an indirect method for quantification of **4**, as in eq 2. Preliminary experiments showed that under the experimental conditions employed, the formation of the product **3** was maximal 50 min after addition of CH_3I and there was no detectable (<5%) decrease in **3** with time after 100 min. Yields were based on analysis 50 min after addition of CH_3I, and are summarized in Table 1.

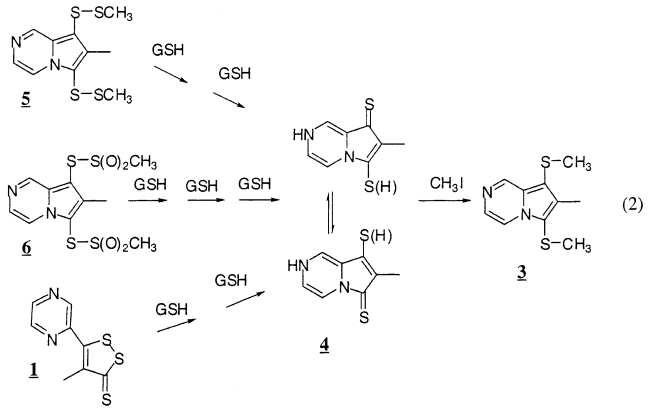

(2)

Kinetics. Both compounds **5** and **6** are relatively stable in buffered aqueous media in the absence of thiols. Ultraviolet/visible spectra are stable for 2 h in the pH region studied, with changes in intensity over the wavelength range 250−600 nm of less than 5%. However the addition of GSH results in a series of spectral changes

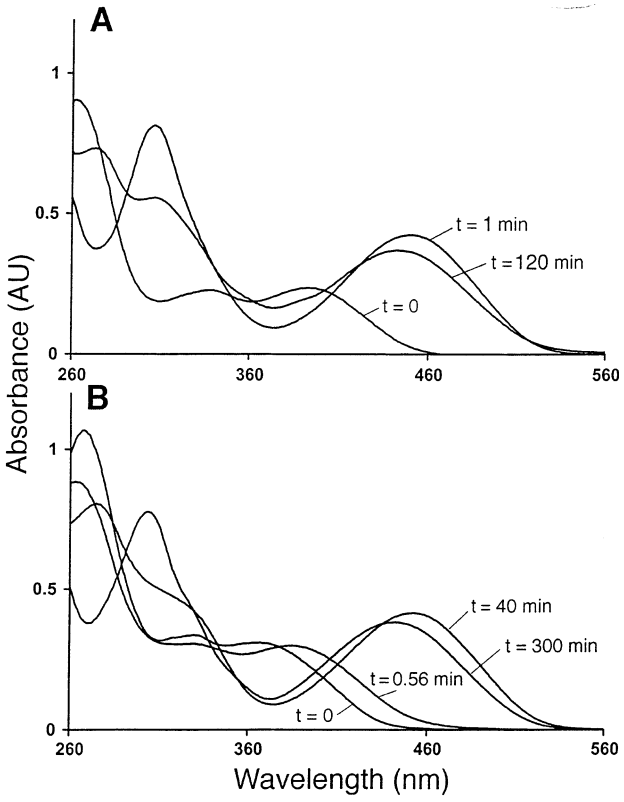

FIGURE 1. UV/vis spectral changes in the reactions of GSH in aqueous solutions with: (A) **5**, pH =1.47, μ = 0.1 M, 15 vol % ethanol; (B) **6**, pH = 2.07, μ = 0.1 M, 4 vol % acetonitrile at 37 °C. Spectra shown are approximate endpoints, reached at the times indicated, for each of the reactions indicated in eq 3.

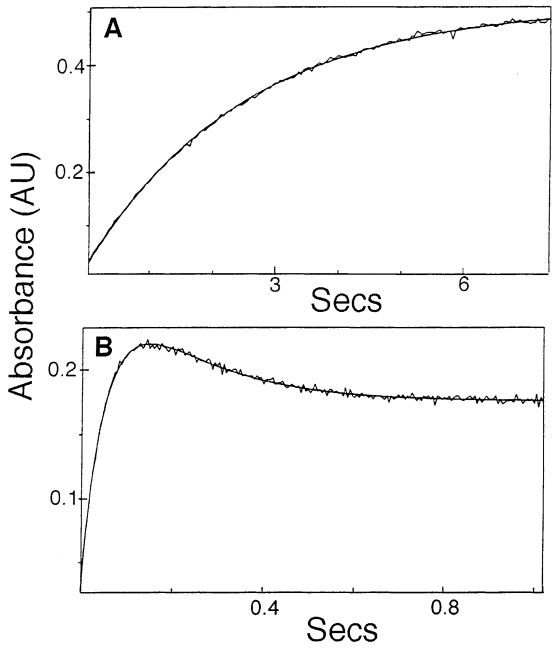

FIGURE 2. Plots of absorbance against time and associated fits to first order (A), or sequential first order (B), expressions in the reaction of GSH with **5** (A) and **6** (B) at 37 °C, in buffered aqueous solutions, 15% ethanol by volume for **5**, 4% acetonitrile by volume for **6**. (A) Reaction of **5** with 0.0061 M GSH in 0.050 M acetic acid buffer (pH = 5.24) monitored at 444 nm. (B) Reaction of **6** with 0.0040 M GSH in 0.050 M tris buffer (pH = 7.78) monitored at 444 nm.

that occur in relatively distinct time windows, as indicated in the spectra of Figure 1. In the case **5**, Figure 1A indicates that two changes are observed, the first characterized by the appearance of a long wavelength band at 450 nm, followed by the second more subtle blue shift of this band and a more marked increase at 260 nm. The times indicated in Figure 1 are generally those at which the change ascribable to that species is finished. In the case of compound **6**, a series of three spectral changes are seen, the first being a subtle red shift of most λ_{max} values, followed by the appearance of the long wavelength band at 450 nm, and finally a blue shift of this band. In this reaction, the latter two changes are qualitatively similar to those observed in the two sequential reactions of compound **5**.

The spectral changes occur consistent with two, in the case of **5**, and three, in the case of **6**, sequential first-order reactions that are each first order in total thiol concentration, as indicated in eq 3. In a number of cases,

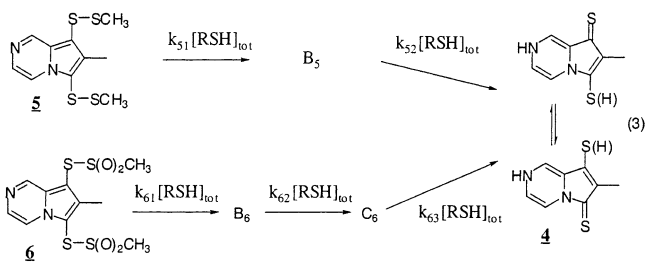

depending on the compound and pH, it was possible to monitor a single spectral change and determine that it was a well-behaved first-order process for 3−5 half-lives as indicated by the data and fit in Figure 2A. Alternatively, when the time window for a spectral change was relatively narrow, two of the processes were monitored; thus in the case of **6**, in a given run, either the first and second or the second and third processes were monitored. The rate constants were derived by fitting to the appropriate expression for first-order or sequential first-order processes, as in Figure 2B, using a commercially available nonlinear least squares routine. Plots of the observed first-order rate constants, for a given process, versus the total thiol concentration were linear (typically $r^2 > 0.99$) with intercept values that were, within experimental error, equal to zero. The slopes of these plots were taken as the observed second-order rate constants, defined by the subscripts in eq 3. Plots of the logarithm of the second-order rate constants for the various reactions (eq 3) as a function of pH are indicated in Figure 3A,B, for compounds **5** and **6**, respectively.

Characterization of Transients. Reactions at various stages of completion were subjected to HPLC with UV/vis and electrospray MS detection. Transient peaks that appeared and disappeared were correlated with the intermediates in eq 3 on the basis of their UV/vis spectra, their order of appearance in the course of reaction, and their difference (when spectrally similar) in retention time from starting material or final product. On the basis of the kinetic results (above), times were chosen so as to maximize the signal from the desired intermediate to obtain mass spectral information. Negative ion electrospray mass spectra of the reactive intermediates, B_5, B_6,

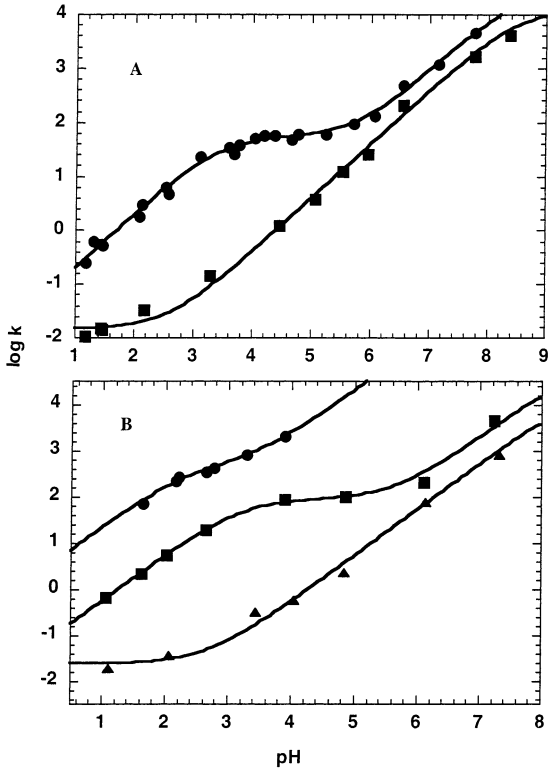

FIGURE 3. Plots of the logarithm of second-order rate constants for the reactions of GSH with **5** (A) and **6** (B) at 37 °C, in buffered aqueous solutions, 15% ethanol by volume for **5**, 4% acetonitrile by volume for **6**. Rate constants are defined for the processes in eq 3 (or also as in Scheme 1): (A) k_{51}, circles; k_{52}, squares. (B) k_{61}, circles; k_{62}, squares; k_{63}, triangles.

and C_6 (eq 3) along with structures assigned for the parent mass signals are given in Figure 4A−C. Nonconventional structures, Figure 4A,C, are used to denote that it is unknown to which pyrrolopyrazinyl sulfur the thio alkyl group is attached—the remaining nonbonded sulfur then bears a formal negative charge.

pK_a Determinations. The UV/vis spectra of both **5** and **6** as well as the final product **4**, eq 3, were observed to vary with pH, consistent with a change in ionization state. With **5** and **6**, this was ascribed to protonation at the low pH of the pyrrolopyrazine ring. Spectral titration (ionic strength = 0.1 M, 37 °C, with solvents containing 15 vol % ethanol for **5** and 4 vol % acetonitrile for **6**), monitored at 300 nm, gave good fits ($r^2 = 0.99$ for **5** and **6**) to the appropriate expression with constants as indicated in eqs 4 and 5 for **5** and **6**, respectively. The pK_a of the parent unsubstituted pyrrolopyrazine has been reported as pK_a = 6.14 in water, 20 °C.[21] In the case of the product **4**, the change is ascribed to the first ionization, as in eq 6. Spectral titration at 450 nm gave a good fit using the constant indicated in eq 6. It is emphasized that this is an *apparent* ionization constant, the tautomeric distribution in eq 6 being unknown. A second spectral change is observed at higher pH ∼ 10, but instability of the product precluded a more quantitative characterization.

EPR Analysis. Experiments were carried out to detect the formation of free radicals by EPR spectroscopy.

(21) Armarego, W. L. F. *J. Chem. Soc.* **1965**, 2778−2787.

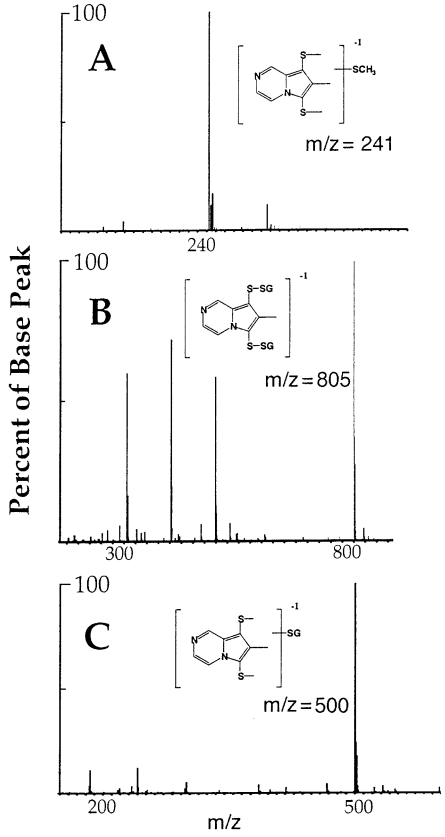

FIGURE 4. Negative ion electrospray LC/MS spectra for the transient species observed in the reaction of GSH with **5** (A) and **6** (B, C) at 37 °C, in buffered aqueous solutions, 15% ethanol by volume for **5**, 4% acetonitrile by volume for **6**. (A) Reaction of **5** (6×10^{-5} M) at 37 °C, 0.051 M acetic acid buffer (pH = 4.22), 0.0010 M GSH, injected onto LC/MS 1 min 30 s after initiation of reaction. (B) Reaction of **6** (7×10^{-5} M) at 0 °C, 0.001 M HCl, 0.0006 M GSH, injected onto LC/MS 1 min 30 s after initiation of reaction. (C) Reaction of **6** (4×10^{-5} M) at 21 °C, 0.001M HCl, 0.0027 M GSH injected onto the LC/MS after 5 min after initiation of reaction.

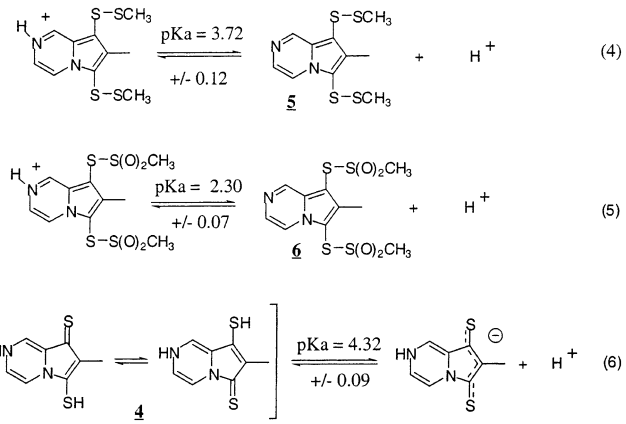

Decomposition of **6** was carried out in the presence of the nitrone spin trap 5,5-dimethyl-1-pyrroline-*N*-oxide. No signal for radicals in excess of background were detected in any of these runs which included the conditions such as those used in kinetic runs, employing 0.02 M phosphate buffer, pH 7.0. Additional experiments were carried out with the same conditions plus 100 μM $FeSO_4$. The limits of detection on the instrument employed is 10 nM

SCHEME 1

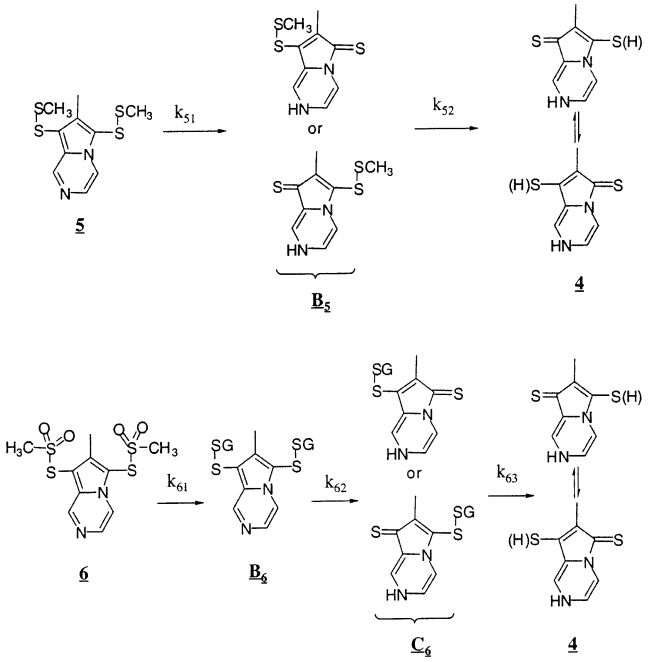

based on the stable 2,2,6,6-tetramethyl-1-piperidinyloxy nitroxyl radical, TEMPO. Thus, the upper limit yield of radicals long-lived enough to be directly or indirectly, by spin trap capture, detected is 0.02%, based on a reaction concentration of starting material of 50 μM.

Discussion

Two Reaction Paths. The changes in UV/vis spectra in the reaction of GSH with **5** and **6** are consistent with the series of transformations summarized in Scheme 1. In both reactions, formation of the long wavelength absorption at ~450 nm is consistent with C=S double bond character in certain intermediates and the product in Scheme 1;[22] more subtle changes are indicative of displacements that give rise to little or no additional C=S character. In the case of **5**, C=S double bond character appears in the initial transformation (Figure 1A), whereas the distinct absorption at 450 nm in the case of **6** only appears in the second phase of the transformation (Figure 1B). The difference is rationalized in Scheme 1. In the case of **5**, glutathione (anion, vide infra) attack occurs at the methane thiol sulfur with the pyrrolopyrazine anion as the leaving group, whereas, in the case of **6**, glutathione attack occurs at the pyrrolopyrazine sulfurs with methyl sulfonate anion as the leaving group. Only in the subsequent (second) reaction in the case of **6**, is the C=S character manifest in the product of glutathione displacement (Figure 1B). The second reaction of **5** (Figure 1A) and the third reaction of **6** (Figure 1B), occur with relatively subtle spectral changes, which are themselves pH dependent, consistent with the replacement of an S−S bond with an ionizable S−H bond, pK_a = 4.32 (eq 6).

Mass spectrometric observations are also consistent with the divergence, between **5** and **6**, summarized in Scheme 1. The observation of the ion m/z = 241, as the product of the first reaction of **5** (Figure 4A), indicates that **5**, in contrast with **6**, is not first transformed to glutathionyl adduct(s) of the pyrrolopyrazine nucleus, a possibility that might not be distinguishable by optical methods. In the case of **6**, the signals at m/z = 805.3 and m/z = 402.3 after the initial reaction (Figure 4B) are as expected for the monoanion and dianion of the diglutathionyl adduct of the pyrrolopyrazine ring. The signals at 500 and 195 are fragment ions as indicated by their predominance, at the expense of m/z = 805.3 and 402.3, as the instrument cone voltage is increased (data not shown). That the second reaction involves attack at one of the glutathionyl sulfurs is indicated by the signal m/z = 500 (Figure 2C). This is not a fragment of a diglutathionyl adduct as indicated by the fact that, first, it is the largest prominent mass observed (compare to Figure 4B) and, second, there is no indication of the dianionic diglutathionyl adduct of m/z = 402.3 in this spectrum (contrast Figure 4B with Figure 4C).

While the reaction path for the disulfide (**5**), with glutathione attack at the methanethiol sulfur, was predictable on the basis of the literature of these reactions,[23−26] the reaction path for the methanesulfonic acid thio ester (**6**), with initial attack at the pyrrolopyrazine sulfur atoms, was not. Generally for disulfide interchange reactions, the dependence of the logarithms of rate constants upon thiolate conjugate acid pK_a, characterized by the quantities β_{lg} (for the leaving group) and β_C (for the central thiol), are more negative for β_{lg} than β_C. This indicates a larger amount of negative charge buildup on the leaving group sulfur than on the central sulfur. Thus the "best leaving group" dictates the course of the reaction. In the case of the sulfonic acid thio ester, there is considerably less known on the competition between the two reaction centers. While methane sulfonic acid methanethiol ester (MMTS) is a well-known cysteine thiomethylating agent (attack at the thiol sulfur atom),[27−29] the pyrrolopyrazine anion is a much less basic anion than the methanethiolate anion which presented the *possibility*, ultimately not observed, of a different reaction course.

The different pathways for conversion of **5** and **6** to **4** could have different manifestations for the biological activity of **5** and **6**. Glutathione conjugates are actively exported by some cell types. To the extent that the ultimate product **4** is biologically active as a phase 2 enzyme inducer, the potency of **6**, relative to **5**, could be diminished by gutathionyl conjugate export pathways.

Kinetics. (a) k_{51}, k_{61}, and k_{62} (Scheme 1). The pH rate profiles (Figure 3A, for k_{51}, and Figure 3B for k_{61} and k_{62}) for these reactions indicate that two terms contribute over the range of pH studied. The "high-pH"

(22) Grimshaw, C. E.; Whistler, R. L.; Cleland, W. W. *J. Am. Chem. Soc.* **1979**, *101*, 1521−1532.

(23) Wilson, J. M.; Bayer, R. J.; Hupe, D. J. *J. Am. Chem. Soc.* **1977**, *99*, 7922−7926.

(24) Freter, R.; Pohl, E. R.; Wilson, J. M.; Hupe, D. J. *J. Org. Chem.* **1979**, *44*, 1771−1774.

(25) Whitesides, G. M.; Lilburn, J. E.; Szajewski, R. P. *J. Org. Chem.* **1977**, *42*, 332−338.

(26) Szajewski, R. P.; Whitesides, G. M. *J. Am. Chem. Soc.* **1980**, *102*, 2011−2026.

(27) Smith, D. J.; Maggio, E. T.; Kenyon, G. L. *Biochemistry* **1975**, *14*, 766−771.

(28) Roberts, D. D.; Lewis, S. D.; Ballou, D. P.; Olson, S. T.; Shafer, J. A. *Biochemistry* **1986**, *25*, 5595−5601.

(29) Klaassen, C. D. *Casarett and Doul's Toxicology, the Basic Science of Poisons*, 5th ed.; McGraw-Hill: New York, 1996.

TABLE 2. Rate and Dissociation Constants Derived for the Reactions of GSH with 5 (k_{51}) and 6 (k_{61} and k_{62}) as Indicated in Scheme 1 at 37 °C[a]

constant	value
k_{51}^{o}	2.11×10^4 M^{-1} s^{-1}
$k_{51}^{H^+}$	6.65×10^6 M^{-1} s^{-1}
$-\log K_{SH}$[b]	3.43
k_{61}^{o}	6.3×10^7 M^{-1} s^{-1}
$k_{61}^{H^+}$	6.2×10^8 M^{-1} s^{-1}
$-\log K_{SH}$[b]	2.36
k_{62}^{o}	3.8×10^4 M^{-1} s^{-1}
$k_{62}^{H^+}$	1.7×10^7 M^{-1} s^{-1}
$-\log K_{SH}$[d]	3.21

[a] Constants defined as in eq 7 for k_{51} (Scheme 1) or with analogous definitions for superscripts for k_{61} and k_{62} (see Discussion—Kinetics). [b] pK_a for the conjugate acid of **5** (see Scheme 1). [c] pK_a for the conjugate acid of **6** (see Scheme 1). [d] pK_a for the conjugate acid of $\mathbf{B}_6$ (see Scheme 1).

extremes of the pH rate profiles for these reactions exhibit slopes approaching 1, consistent with the reactive species being the glutathione anion with neutral pyrrolopyrazine derivatives. With decreasing pH, each of the profiles exhibits an upward break, most distinctly in the case of k_{51} and k_{62}, followed by a downward break. This is consistent with reaction of the glutathione anion with the more electrophilic protonated pyrrolopyrazine ring.[23−26] Protonation of **5** and **6** in this region is expected on the basis of the measured pK_a values of 3.5 and 2.5, respectively (eqs 4 and 5, respectively) The kinetically ambiguous possibility that the upward break is due to the onset of the reaction of neutral thiol with neutral substrates is untenable due to the subsequent downward break at lower pH—the more reactive (see below) protonated substrate would be more reactive with the neutral thiol, resulting in a subsequent upward break.

An example of the required two term rate law is given for k_{51} in eq 7. The rate expression is derived in terms of total substrate and total thiol concentration, where K_{GSH} and K_{SH} are the ionization constants for the thiol group on GSH and the dissociation

$$k_{51} = \frac{k_{51}^{o}}{\left[1 + \frac{[H^+]}{K_{GSH}}\right]\left[1 + \frac{[H^+]}{K_{SH}}\right]} + \frac{k_{51}^{H^+}}{\left[1 + \frac{[H^+]}{K_{GSH}}\right]\left[1 + \frac{K_{SH}}{[H^+]}\right]} \quad (7)$$

constant for the conjugate acid of the substrate, respectively; and k_{51}^{o} and $k_{51}^{H^+}$ are constants for the reactions of the anion of GSH with the neutral and protonated substrates, respectively. Expressions for the reactions k_{61} and k_{62} are strictly analogous containing the relevant dissociation constants and the pairs of kinetic constants; k_{61}^{o} and $k_{61}^{H^+}$ for reaction k_{61}, and k_{62}^{o} and $k_{62}^{H^+}$ for reaction k_{62}, where the superscript "o" is for the reaction of the neutral substrate while the superscript "H^+" is for reaction of the protonated substrate. Best fits to the data for these reactions in Figures 1 and 2, indicated by the solid lines, were obtained using the measured pK_a of GSH and allowing the two rate constants and the dissociation constant of the substrates to vary. These constants are summarized in Table 2. In the case of **5** and **6**, the values of the pK_{SH} are in reasonable agreement with the measured values, eqs 4 and 5.

The kinetic form of eq 7 bears similarity to what has been observed previously in the displacements at dipyridyl disulfides that undergo changes in ionization state (eq 8) in the pH region studied.[22] The neutral form, eq 8,

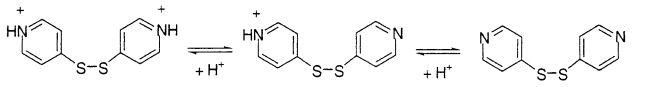

(8)

is a factor of 2−3 more reactive than the neutral disulfides here (k_{51}^{o}, k_{62}^{o}). Rate constants of the neutral disulfides studied here are also not dissimilar to those reported for the well-studied bis-dithionitrobenzoic acid for which the second-order rate constants for reactions with various alkanethiolates of pK_a = 7−9 are in the range of 10^4−10^5 M^{-1} s^{-1}.[23,25] The monoprotonated form of the dipyridyl disulfide (eq 8) is most similar in reactivity to the protonated disulfides studied here, being a factor of 3 less reactive than the diglutathionyl adduct ($\mathbf{B}_6$, Scheme 1, $k_{62}^{H^+}$ in Table 2).

The assignment of the rate constant k_{61} (Scheme 1) as that for displacement of both methanesulfonate groups is based on the assumption that substitution at one of the pyrrolopyrazine sulfurs by glutathione does not measurably alter the reactivity at the other sulfur. Support for this assumption is found in the comparison of the values of k_{61}^{o} and $k_{61}^{H^+}$ which shows that protonation of the pyrrolopyrazine ring causes only a 10-fold increase in reactivity; it is thus reasonable that the much smaller change in electron density due to substitution of the methane sulfonate group by glutathione would likely have a negligible effect on reactivity at the other sulfur. The slowest first-order process observed in this reaction, at the lowest glutathione concentration and the lowest pH had a half-time of ~6 s, with the initial time point being 0.02 s. The spectrum at the initial time point was virtually indistinguishable from starting material. Thus there is no spectroscopically distinguishable change that precedes the initial first-order process.

In the strictest sense though it is not possible to rule out that there are two kinetically different process, but that the first is spectroscopically undetectable.

The reactivity of the methylsulfonate thioester is modestly larger than what has been reported for MMTS.[28] The rate constant k_{61}^{o} for reaction with glutathione anion with **6** is 40-fold larger than that for the reaction of mercaptoethylamine anion with MMTS. The nucleophiles in these reactions are of comparable basicity, pK_a(GSH) = 8.85 and pK_a(mercaptoethylamine) = 8.46. The value of $\beta_{nuc} = 0.36$ has been measured for MMTS, so that the difference in basicity, which predicts a 32% larger rate constant for glutathione if all else were equal, cannot explain the much larger observed difference. The rate constant $k_{61}^{H^+}$ is larger still by another factor of 10. The larger magnitudes of k_{61}^{o} and $k_{61}^{H^+}$ in comparison with what is observed for a roughly comparable thiolate with MMTS are both consistent with the previous observations that decreasing electron density in the central thiol enhances reactivity in contrast to simple S_N2 reactions at carbon centers.[23−26]

(b) k_{52} and k_{63} (Scheme 1). These reactions also involve two kinetic terms in the pH range studied. The spectra of intermediates $\mathbf{B}_5$ and $\mathbf{C}_6$ (Scheme 1) exhibit

no changes as a function of pH in the pH range studied. The near unit slopes in the higher pH region indicate the requirement for the glutathione anion. At the lowest values of pH, pH ~ 1, the values of the rate constants k_{52} and k_{63} are larger than predicted by a line of unit slope based on the data at pH > 4 by factors of about 10 and 30, respectively. These deviations are larger than can be attributed to experimental error in the determination of the rate constants and are ascribed to the onset of a "pH independent" reaction. It is unclear whether this represents a reaction of thiol anion with a protonated form of the intermediates or simply a reaction of the thiol with the neutral intermediates. For simplicity and as the ionization constants for the intermediates are unknown, the rate expression is written in eq 9 in the case of k_{52}, derived in terms of total thiol concentration and in terms of the latter possibility, where $k_{52}^{S^-}$ and k_{52}^{SH} are constants for the pH dependent and pH independent reactions, respectively.

$$k_{52} = \frac{k_{52}^{S^-}}{\left[1 + \frac{[H^+]}{K_{GSH}}\right]} + \frac{k_{52}^{SH}}{\left[1 + \frac{K_{GSH}}{[H^+]}\right]} \qquad (9)$$

A strictly analogous expression applies in the case k_{63}, with the same superscripts representing the analogous kinetic processes. Best fits to these rate expressions appear as the solid lines in Figures 1 and 2 using the constants $k_{52}^{S^-} = 1.2 \times 10^4\ M^{-1}\ s^{-1}$, $k_{52}^{SH} = 0.0143\ M^{-1}\ s^{-1}$, $k_{63}^{S^-} = 1.61 \times 10^4\ M^{-1}\ s^{-1}$, and $k_{63}^{SH} = 0.024\ M^{-1}\ s^{-1}$.

EPR: No Evidence Requiring Radicals. Experiments, using the nitrone spin trap DMPO, were carried out to detect and trap either radical reactive intermediates or products formed in the decay of **6** and failed to detect signals ascribable to such radicals. On the basis of the instrument sensitivity using the stable free radical TEMPO, an upper limit of 0.02% of the reaction flux was trapped in this way. The maximum percent of reaction that could have occurred through trappable radicals depends on the efficiency of the trap. Under conditions similar to those used in these experiments, the agent DMPO traps the highly reactive hydroxyl radical with an efficiency of between 10 and 20% and with a rate constant that is nearly diffusion controlled.[30] It is expected that thiyl radicals are likely less reactive and more efficiently trapped than hydroxyl radical,[31] but the most conservative conclusion, based on the above minimum trapping efficiency of 10%, is that less than 0.2% of the reaction occurs through radicals that are as reactive or less reactive than the hydroxyl radical.

More extensive experiments are currently under way to determine conditions whereby the observed products of the reaction might give rise to oxygen-derived or other free radicals and will be reported upon in due course.

Summary. Compounds **5** and **6** react with GSH to give **4** in nearly quantitative yields by the pathways indicated in Scheme 1. These reactions occur at GSH concentrations in the millimolar range, which is comparable to GSH concentrations in a number of cell types including importantly liver, a detoxifying organ rich in inducible phase 2 enzymes. Though it cannot yet be excluded that some obfuscatory enzymatic processes may intervene, this study establishes that it should now be possible to test directly if **4** is indeed a phase 2 enzyme inducer by employing the prodrugs **5** and **6**.

JO020588N

(30) Carmichael, A. J.; Makino, K.; Riesz, P. *Radiat. Res.* **1984**, *100*, 222−234.

(31) Halliwell, B.; Gutteridge, J. M. *Free Radicals in Biology and Medicine*, 3rd ed.; Oxford Science Publications: Oxford, U.K., 1998.